infrastructures

MDPI

Article

Experimental Assessment of Geocell-Reinforced Sandy Subgrades Under Traffic-Induced Dynamic Loading

Mo'men Ayasrah [1,2,*], Hongsheng Qiu [1,*], Mohammed Y. Fattah [3], Wallaa B. Mohammed Redha [4] and Bin Zhu [1]

[1] School of Transportation and Logistics Engineering, Wuhan University of Technology, Wuhan 430063, China
[2] Department of Civil Engineering, Faculty of Engineering, Al Al-Bayt University, Mafraq 25113, Jordan
[3] Civil Engineering Department, University of Technology-Iraq, Baghdad 10066, Iraq; 40011@uotechnology.edu.iq
[4] Civil Engineering Department, University of Karbala, Karbala 56001, Iraq; walaa.b@uokerbala.edu.iq
* Correspondence: ayasrahmomen@whut.edu.cn (M.A.); 2755@whut.edu.cn (H.Q.)

Abstract

This study performs a comprehensive experimental analysis of the dynamic response of geocell-reinforced sandy subgrades exposed to traffic-induced loading. A series of laboratory tests were performed using a custom-manufactured loading apparatus capable of creating monitored dynamic waveforms representative of vehicular traffic. A steel strip footing was assigned on both unreinforced and geocell-reinforced sandy beds to evaluate the implementation of the reinforcement in attenuating transmitted vertical stresses and surface settlements. The influence of key parameters, among which were load amplitude (0.5 and 1.0 tons), loading frequency (0.5, 1.0, and 2.0 Hz), and relative density of sand (30% loose and 60% medium), was systematically examined. The applied dynamic loading was based on a force-controlled sinusoidal waveform with constant amplitudes and frequencies, which corresponded to low-frequency harmonic cyclic loading in the case of traffic-induced quasi-static effects. Therefore, the experimental results indicate that geocell reinforcement reduces the transmitted vertical dynamic stress by up to 45% and reduces surface settlement by about 60% compared to unreinforced sand. However, the heightening efficiency decreases with loading frequency, the amplitude of the load, and the relative sand density. Thus, the findings are important in highlighting the capacity of geocell systems to enhance the longevity and efficiency of sand substrates when the systems are subjected to low-frequency harmonic cyclical loading conditions pertaining to traffic-induced quasi-static influences.

Keywords: geocell reinforcement; dynamic traffic load; sandy soil; surface settlement

Check for updates

Academic Editor: Giuseppe Loprencipe

Received: 11 December 2025
Revised: 18 January 2026
Accepted: 23 January 2026
Published: 26 January 2026

Copyright: © 2026 by the authors. Licensee MDPI, Basel, Switzerland. This article is an open access article distributed under the terms and conditions of the Creative Commons Attribution (CC BY) license.

1. Introduction

The ability of a subgrade to withstand the stresses and vibrations caused by traffic is a critical factor in the dynamic performance of transportation infrastructure. Modern railway and highway networks, especially those built on sandy or weak granular soils, are progressively exposed to higher traffic speeds, heavier axial loads, and more frequent loading cycles. These factors exacerbate the dynamic stresses transmitted to the soil, resulting in excessive deformation, stiffness degradation, and long-term serviceability problems. Ground vibrations from traffic can also have adverse effects on adjacent structures, sensitive equipment, and urban communities [1–3]. Traditional solutions for improving subgrades,

such as deep soil modification or thick granular replacement, are often costly and difficult to implement within existing transport corridors.

Traditional vibration mitigation measures, such as backfilled barriers and open trenches made of materials like concrete, bentonite, and expanded polystyrene (EPS) foam [4,5], have shown limited effectiveness and often suffer from problems related to ease of implementation, long-term stability, and cost. Among the various types of geosynthetic materials, geocells possess unique advantages due to their three-dimensional, honeycomb-like structure. When brushed and filled with soil, these interconnected cells provide a closed space that completely encloses the filler material, generating annular stress within the cell walls and enhancing the negative resistance of adjacent cells. This containment mechanism significantly increases the apparent stiffness and shear resistance of the composite mass (soil–geocell), prevents lateral soil spread, and distributes vertical traffic loads over a wider impact area [6].

Consequently, geocell reinforcement has been shown to improve bearing capacity, reduce cracking, and enhance the response of weak layers under static and repetitive loads [7–14]. Compared to planar reinforcement materials such as geogrids, geocells offer better spatial containment and greater energy dissipation due to their closed three-dimensional structure.

However, most previous research has concentrated mostly on static behaviour, such as plate loading tests [15], large-scale triaxial tests [16], and shear resonance studies [17]. Although several studies have addressed dynamic aspects and indicated improvements in elastic response, normal frequency, and damping capacity as a result of using ground cells [18–22], the vast majority have relied on simplified harmonic or periodic loading models. These idealized models do not reflect the irregular, time-varying, and multi-frequency nature of actual vehicle motion and therefore fail to accurately represent the true dynamic behavior of the reinforced base sand layers. Based on this, this paper will explore the frequency- and amplitude-dependent dynamic behavior of geocell-reinforced sand under the time-dependent loading conditions that are more representative of the excitations created by vehicles. Such a practice provides a new experimental model for measuring the interactive effect of loading frequency, load amplitude, and soil density on the transmission of dynamic stresses and settlement in geocell-reinforced sand layers.

As transportation systems, particularly older railway bed layers, continue to face increasing dynamic demands, replacing granular soils with geosynthetics has become a promising approach for stress dissipation and long-term performance improvement [23–25]. Although geocells have been explained to have the ability to reduce dynamic displacements, minimize deformations, and extend the service life of weak subgrades [26,27], the dynamic performance of geocell-reinforced sand under traffic-induced low-frequency loading conditions remains insufficiently understood. This knowledge gap persists mainly because many experimental studies have relied on simplified or idealized loading assumptions that do not fully capture the influence of loading frequency and amplitude on reinforced sand behavior.

To bridge this gap, the current study employs a specially designed loading device capable of generating controlled dynamic loads at varying amplitudes and low-frequency ranges representative of traffic-induced quasi-static loading conditions. Through a systematic series of laboratory tests on loose and medium-dense sandy soils, the study evaluates the effectiveness of geocell reinforcement in reducing vertically transmitted dynamic stresses and surface settlement under low-frequency harmonic cyclic loading. Consequently, the following sections present the test setup, loading system, soil properties, instrumentation, and test procedures used to assess the dynamic behavior of geocell-reinforced and unreinforced sand layers within the investigated frequency range.

2. Materials Used

2.1. Sandy Soil

The sand used in this study was oven-dry clean sand, and its physical properties were determined in accordance with relevant ASTM standards. Based on the Unified Soil Classification System (USCS), the material is classified as poorly graded sand (SP). The particle size distribution curve of the sand is illustrated in Figure 1, and the corresponding index properties are summarized in Table 1.

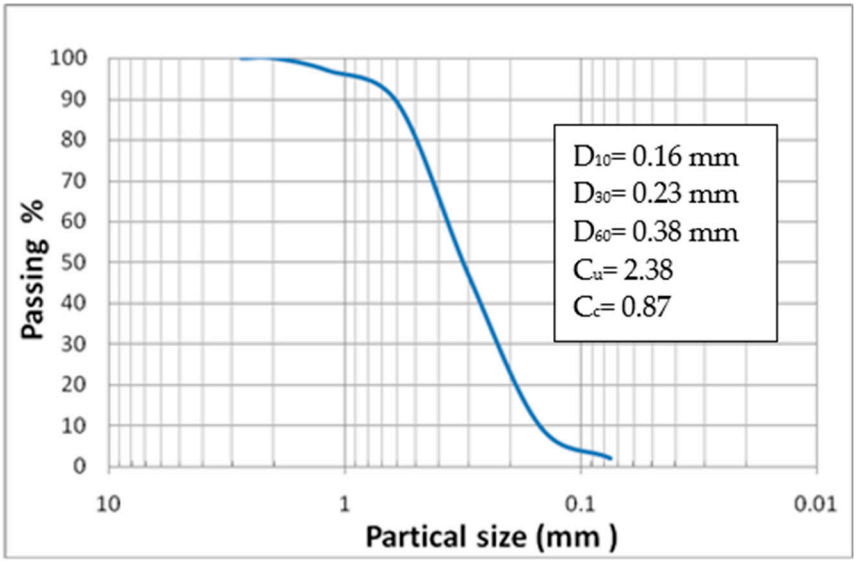


Figure 1. Grain-size distribution curve of sand.

Table 1. Physical and index properties of the sandy soil.

Soil Property	Value	Test Standard
Specific gravity	2.64	ASTM D 854 [28]
Curvature coefficient (Cc)	0.87	ASTM D 422 [29] and ASTM D 2487 [30]
Uniformity coefficient (Cu)	2.37	
Unified Soil Classification System (USCS)	SP	
Minimum void ratio	0.38	-
Maximum void ratio	0.63	-
Minimum dry unit weight (kN/m^3)	15.32	ASTM D 4253 [31]
Maximum dry unit weight (kN/m^3)	18.82	ASTM D 4254 [32]
Friction angle (at RD = 30%)	32°	ASTM D 3080 [33]
Friction angle (at RD = 60%)	38°	

2.2. Geocell

The geocell reinforcement used in this study was locally fabricated from planar polymeric strips that were stitched together at regular intervals to form a three-dimensional honeycomb structure. The resulting system is a non-perforated, flexible geocell suitable for confinement of sandy soils. The cell height was maintained at 25 mm. The pocket size (d) of the geocell was defined as the diameter of an equivalent circular area corresponding to the pocket opening area (Ag), as illustrated in Figure 2, and was computed using the following expression.

$$d = \sqrt{\frac{4A_g}{\pi}} \quad (1)$$

A constant pocket size, d = 70 mm, was employed throughout the experimental program. The ratio of the geocell pocket size to the footing width (d/B) was fixed at 0.7,

which lies within the optimal range of 0.7–0.8 recommended by Dash et al. (2001) [34] for achieving maximum improvement in load–deformation response. Moreover, geocell reinforcement was locally performed using high-density polymeric strips (polymers of high-density polyethylene, HDPE) cut out of planar sheets. The honeycomb structure was constructed by stitching the strips with a high-strength polymer thread with a thickness of approximately 1.2 mm in the intermittent places, that is, with a space between them of approximately 20 mm. The geocell was perforated and flexible. The stitched joints showed sufficient tensile continuity at the levels of loading imposed without any rupture or slipping of the joints when tests were not performed directly on tensile and seam strength. Depending on the strip material and geometry, the tensile stiffness of the geocell strips was estimated to be in the order of 80 kN/m, similar to lightweight commercial geocell products applied in laboratory-scale experimental research.

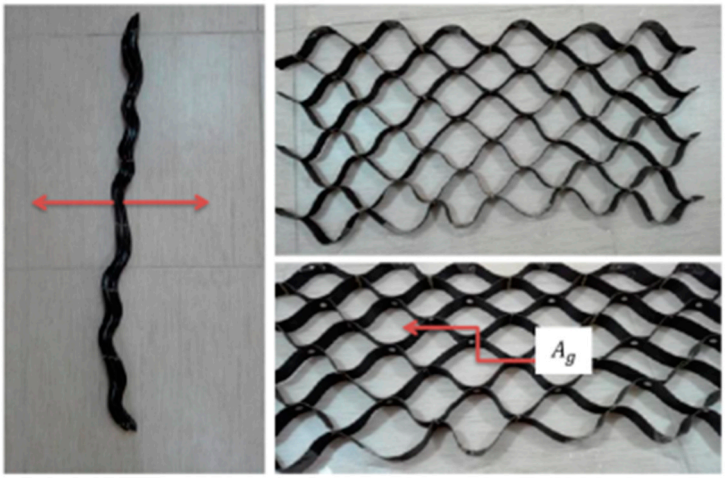


Figure 2. Geocell mattress used in experiments.

2.3. Data Acquisition System and Test Devices

The experimental setup was equipped with a data acquisition system developed to automatically record surface settlement using a Programmable Logic Controller (PLC). An earth pressure cell was embedded within the soil layer at a depth of 200 mm equivalent to twice the footing width to measure the vertical stress transmitted to the subgrade. A general view of the laboratory test arrangement is shown in Figure 3. The experiments were performed inside a rigid test tank measuring 800 mm × 800 mm × 800 mm, fabricated from 6 mm thick cast iron plates. Structural rigidity of the tank was also provided by reinforcing the sides of the tank with three stiff steel U-sections, as shown in Figure 3. The edges of the geocell mattress were left with a small clearance of 25 mm between them and the rigid side walls of the tank, and this created a B/tank width ratio of about 0.94. This discontinuity reduced the effects of the boundary, and the impact of the rigid walls on the distribution of stress and settlement, particularly at the center of the footing, was negligible [35]. The tank was mounted on a loading frame connected to an automated hydraulic jack used to apply dynamic loading. Traffic-induced dynamic loads were simulated by applying vertical cyclic loads through a steel loading plate positioned on the soil surface. A rectangular steel plate with dimensions of 30 mm (thickness) × 100 mm (width) × 750 mm (length) was used for this purpose, as shown in Figure 4. In addition, the axial loading system consisted of two major parts:

1. Hydraulic jack system: The piston cross-sectional area and length are 176 mm^2 and 1300 mm, respectively. The system is capable of applying a maximum load of 4 tons, as shown in Figure 3.

2. Hydraulic control system: This control device includes a precision control valve used to regulate the magnitude and frequency of the applied dynamic force. Also, the control device includes a system responsible for the dynamic loading application and the piston movement.

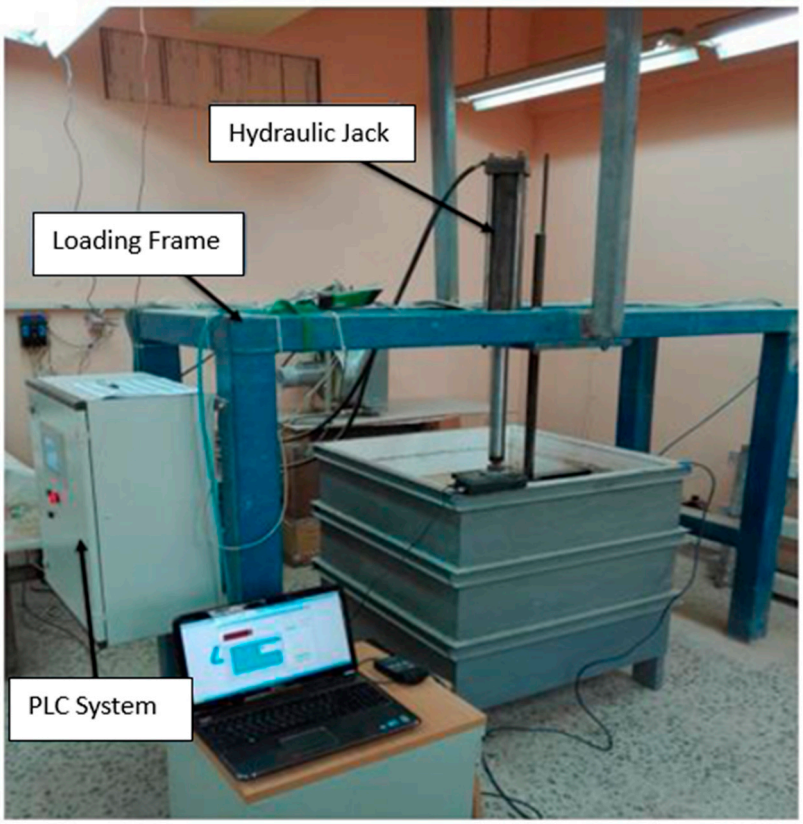


Figure 3. Overall view of the experimental system.

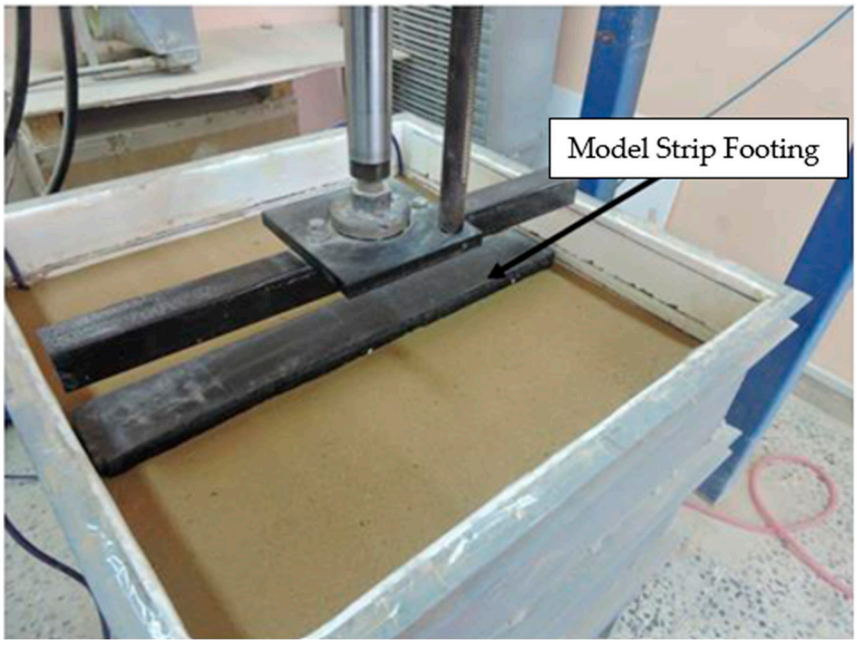


Figure 4. Steel strip footing model used in the laboratory tests.

2.4. Model Preparation and Testing Program

The calculated weight of dry sand required for each test was poured into the test tank in layers of 100 mm thickness to maintain a uniform deposit. Each layer was compacted to achieve the desired relative density of 30% (loose) or 60% (medium). Compaction was conducted by a square steel plate with a 200 mm width and a thickness of 10 mm, which was uniformly filled to tamped consistent density throughout the sand bed. After finishing the last layer, the surface was levelled using a sharp-edged ruler to obtain a smooth and uniform top surface. Then, the strip footing was positioned directly on the sand surface. The main steps of the sample sand deposit preparation are illustrated in Figure 5.

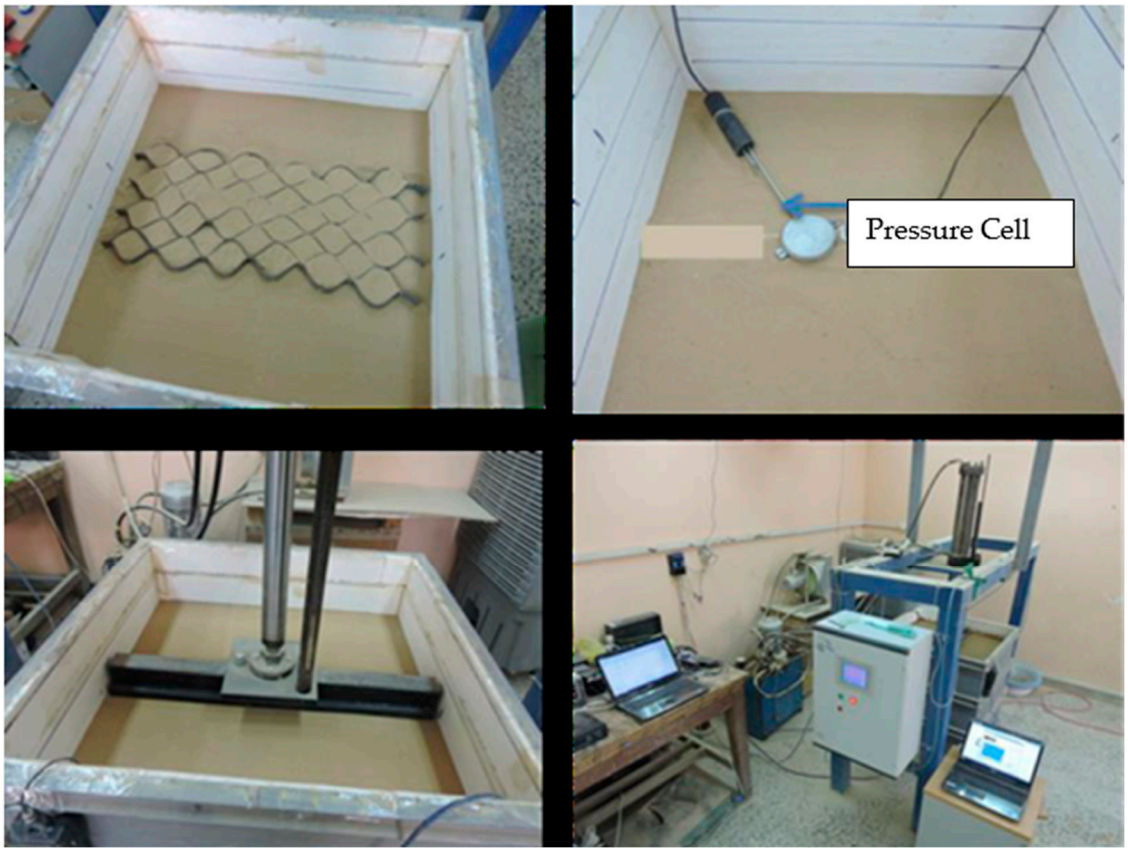


Figure 5. Test model preparation.

A total of 48 laboratory model tests were established to understand the response of geocell-reinforced sand under dynamic loading. Therefore, two test series were conducted corresponding to the two relative densities (30% and 60%), which correspond to loose and medium sand, respectively. It is worth mentioning that, for comparison purposes, all models were tested under various load amplitudes and frequencies used to assess both the unreinforced and geocell-reinforced sand beds.

In the reinforced tests, the geocell reinforcement layer was placed along the full length of the tank with a small clearance from the sidewalls left to reduce boundary effects. The geocell width was maintained at about 3.2 times the width of the loading plate in all tests.

Dash et al. (2001) [34] reported that the optimum depth of geocell placement is 0.1 B from the bottom of the footing. Hence, in the present exploration, the geocell was positioned at a depth of 0.1 B beneath the steel plate. This place coincides with the zone of the highest stress and strain concentration through dynamic loads, where geocell confinement and redistribution of pressure are most influential. This leads to an increase in the degree of stiffness and a reduction in permanent deformation at repeated loads. Figure 6 shows the

geometry of the test configuration. For each test case, the dynamic loading was applied for a fixed duration of 1000 s. The total number of loading cycles (N) was determined based on the selected loading frequency according to N = f × T, where f is the loading frequency (Hz) and T is the total loading duration (s). Accordingly, the applied loading resulted in 500, 1000, and 2000 cycles for loading frequencies of 0.5, 1.0, and 2.0 Hz, respectively. The responses of settlement and vertical pressure were continuously acquired during the loading period in the form of time histories. The maximum values were then removed from the measured signals to facilitate comparison of the responses.

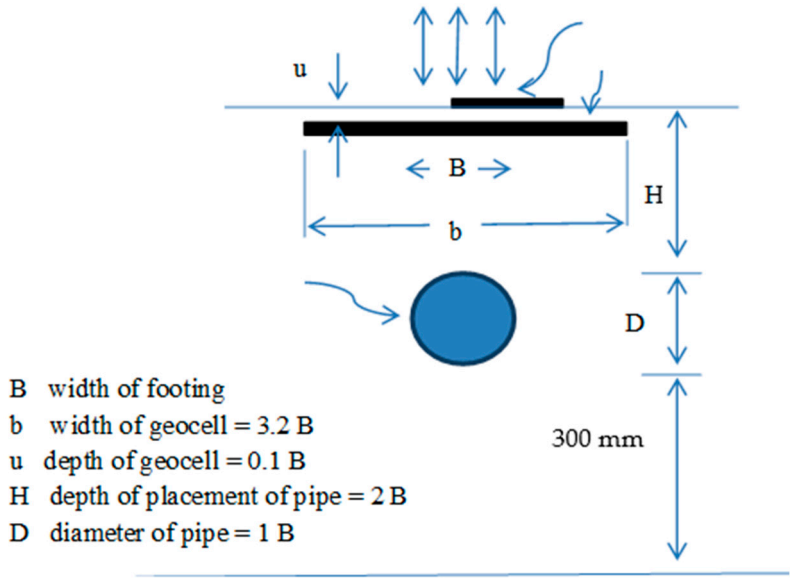


Figure 6. Geometry of the experimental test configuration.

3. Results

3.1. Effect of Load Amplitude on the Pressure Transmitted to the Soil Subgrade

Figures 7–10 explain the difference in the vertical pressure transmitted to the soil subgrade with time under different load amplitudes. Overall, the transmitted vertical pressure increases with increasing load amplitude.

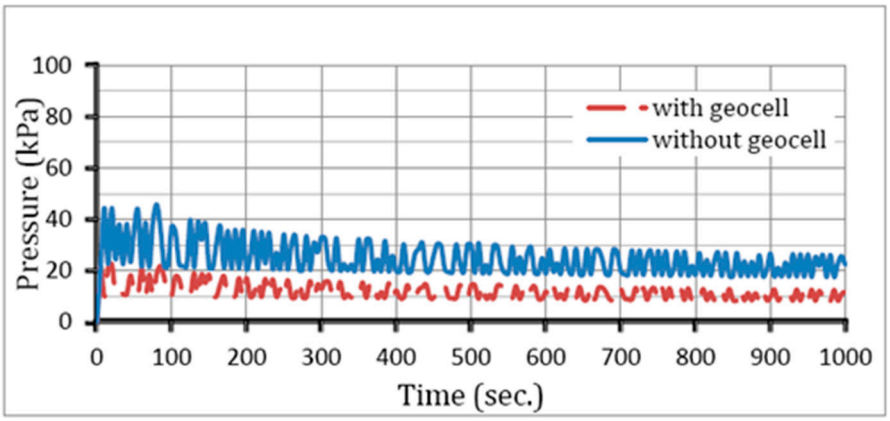


Figure 7. Variation in vertical dynamic pressure for a load amplitude of 0.5 ton, loading frequency of 0.5 Hz, and R.D. of 30%, for tests on unreinforced and geocell-reinforced sand.

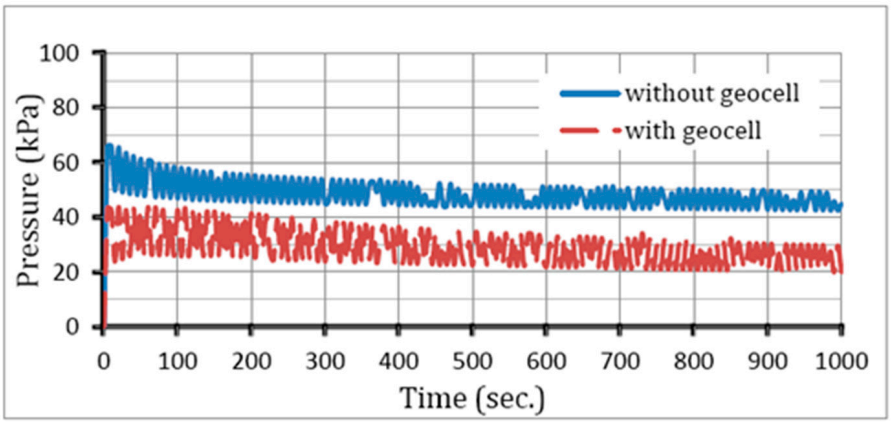


Figure 8. Variation in vertical dynamic pressure for a load amplitude of 1.0 ton, loading frequency of 0.5 Hz, and R.D of 30%, for tests on unreinforced and geocell-reinforced sand.

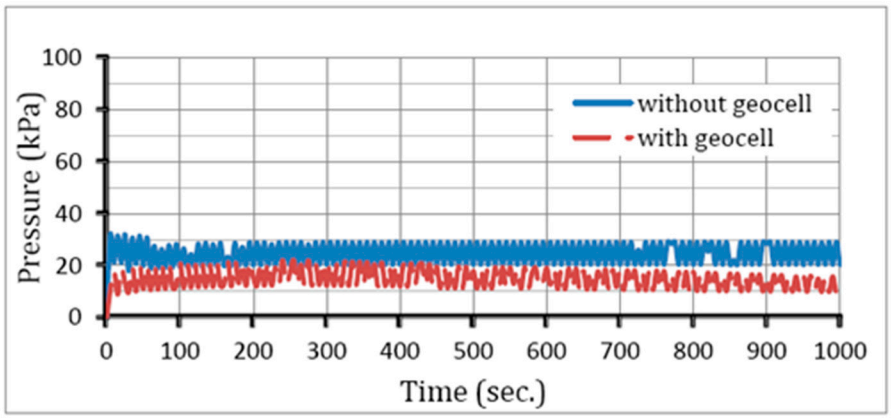


Figure 9. Variation in vertical dynamic pressure for a load amplitude of 0.5 ton, loading frequency of 0.5 Hz, and R.D of 60%, for tests on unreinforced and geocell-reinforced sand.

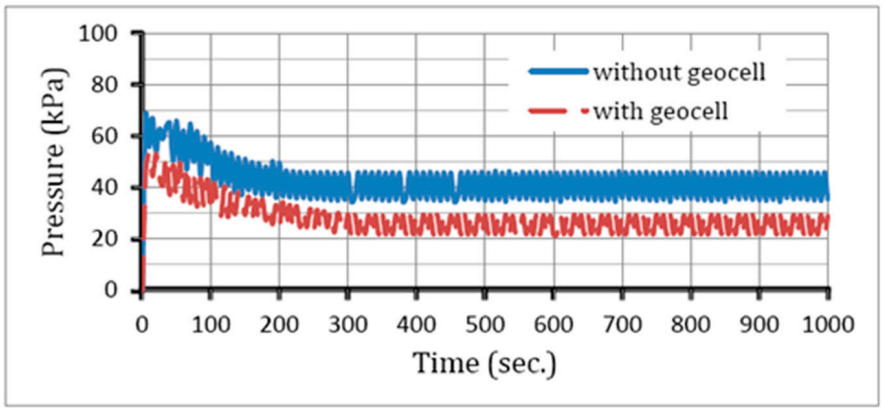


Figure 10. Variation in vertical dynamic pressure for a load amplitude of 1.0 ton, loading frequency of 0.5 Hz, and R.D. of 60%, for tests on unreinforced and geocell-reinforced sand.

Comparison of the pressure results with and without geocells indicates that, in loose sand, geocell reinforcement can reduce the transmitted dynamic pressure by approximately 48% when the load amplitude equals 0.5 tons, while the reduction decreases to 35% when the load amplitude becomes 1 ton. Moreover, in medium sand, the corresponding reductions are 30% and 25%, respectively. It can be concluded that the efficiency of geocell reinforcement decreases as the applied dynamic load amplitude increases.

The findings agree with the reinforcement mechanisms described by Tafreshi and Dawson (2010) [36], who suggested several contributing reasons:

- Hoop tension and confinement: The geocell walls mobilize hoop action that prevents lateral displacement of the infill, thereby increasing the shear strength of the composite soil geocell system.
- Three-dimensional load transfer: Vertical stress applied to the infill induces horizontal active pressure on the perimeter of the cell, and friction at the infill wall interface transfers load to adjacent cells, creating a 3D load-sharing mechanism.
- Passive resistance of surrounding cells: Cells adjacent to the loaded zone mobilize additional passive resistance due to lateral strains, further enhancing the system's stiffness.
- Formation of a stiff composite slab: Together, these mechanisms cause the reinforced layer to extend as a stiff slab with high flexural stiffness, providing efficient load spreading and decreasing vertical stress transmission.

The combined effect of these mechanisms explains the substantial reduction in transmitted dynamic pressure observed in both loose and medium sands.

3.2. Effect of Load Frequency

Figures 11–14 present the variation in vertical pressure transmitted at the measurement location beneath the loading area in loose and medium sand for different loading frequencies. For the same load amplitude, increasing the frequency from 0.5 Hz to 2.0 Hz results in an increase of approximately 43% in the transmitted vertical pressure for both the 0.5-ton and 1-ton load amplitudes. This behavior can be attributed to the fact that increasing the loading frequency intensifies the applied load within a limited time interval, leading to higher cyclic stresses and, consequently, greater vertical pressure transmitted to the subgrade beneath the loading plate. These findings are consistent with the observations reported by Al-Ameri (2014) [37] and Fattah et al. (2016) [38], who observed that the induced dynamic stress (σdy) increased with the operating frequency (ωr) for all tested soil densities. This can be attributed to the fact that the geocell layer can distribute loads. When sand is added to the geocell pockets, the system provides a rigid platform that distributes the stress over a larger area, rather than passing it directly under the loaded area.

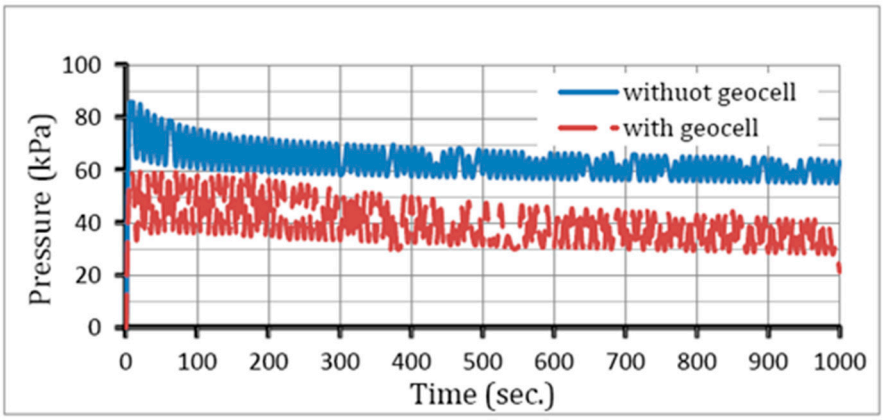


Figure 11. Variation in vertical dynamic pressure for a load amplitude of 1.0 ton, loading frequency of 1 Hz, and R.D. of 30%, for tests on unreinforced and geocell-reinforced sand.

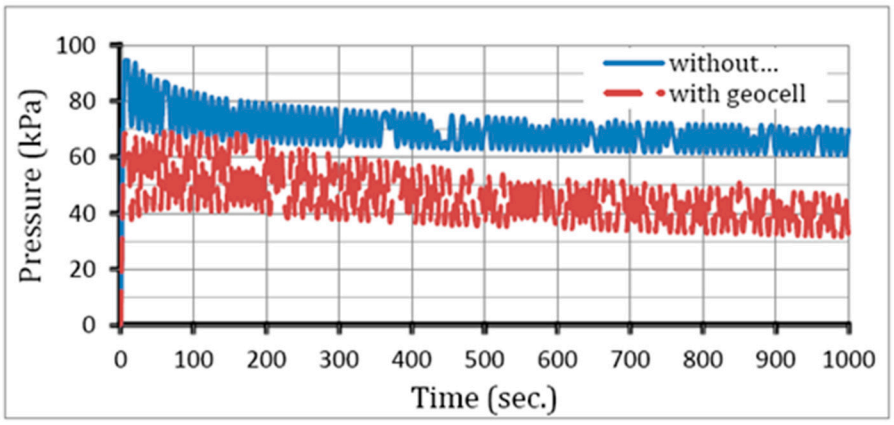


Figure 12. Variation in vertical dynamic pressure for a load amplitude of 1.0 ton, loading frequency of 2 Hz, and R.D. of 30%, for tests on unreinforced and geocell-reinforced sand.

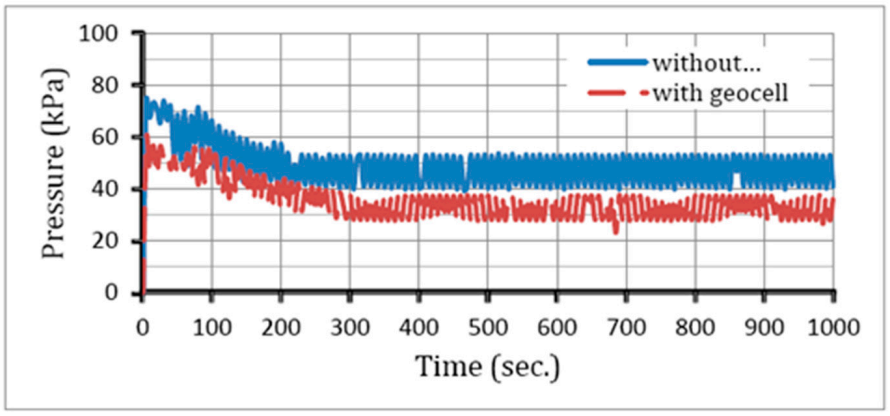


Figure 13. Variation in vertical dynamic pressure for a load amplitude of 1.0 ton, loading frequency of 1 Hz, and R.D. of 60%, for tests on unreinforced and geocell-reinforced sand.

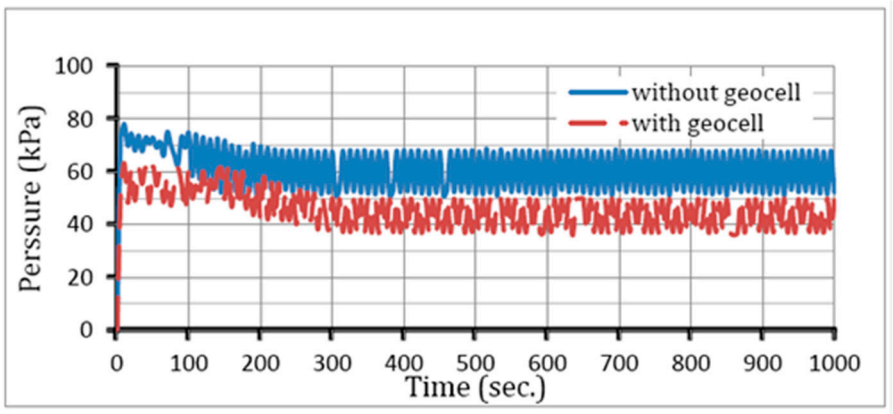


Figure 14. Variation in vertical dynamic pressure for a load amplitude of 1.0 ton, loading frequency of 2 Hz, and R.D. of 60%, for tests on unreinforced and geocell-reinforced sand.

The maximum readings of transmitted dynamic stresses were extracted for all test conditions, and the variation between the maximum stress and loading frequency is given in Figure 15, which highlights the strong frequency-dependent nature of dynamic stress amplification.

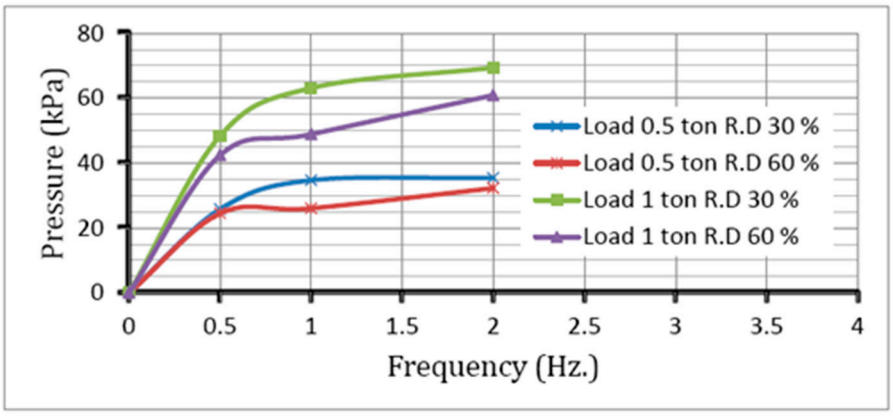


Figure 15. Relationship between vertical pressure and load frequency to the soil subgrade for various amplitudes and relative densities.

3.3. Effect of Dynamic Load on the Surface Settlement

3.3.1. Effect of Load Amplitude

Figures 16–19 show the response of the time settlement of the tested models in both loose and medium sand. In all cases, the surface settlement increases with increasing load amplitude, and the settlement rate accumulation is noticeably higher in loose sand compared with medium sand. This variation is attributed to the lower stiffness and greater particle mobility in loose sand, which allows for higher deformation under cyclic loading.

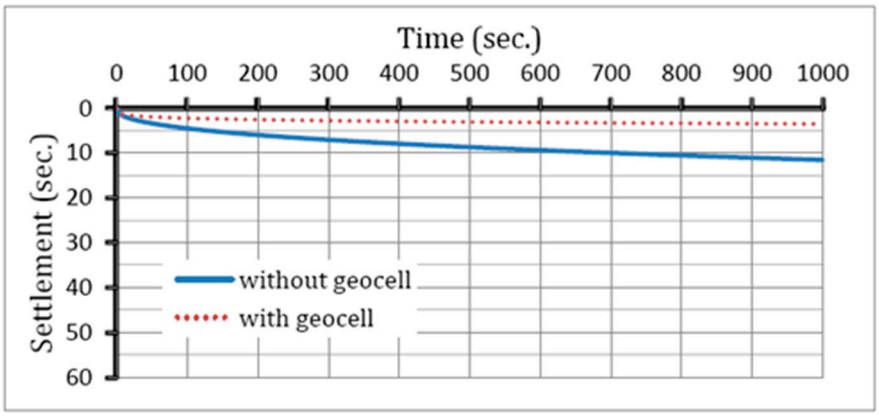


Figure 16. Surface settlement variation with time for a load amplitude of 0.5 ton, loading frequency of 0.5 Hz, and R.D. of 30%, for tests on unreinforced and geocell-reinforced sand.

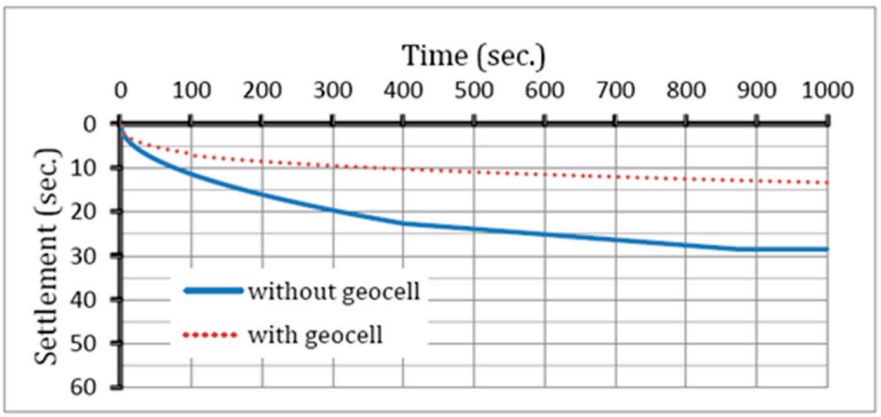


Figure 17. Surface settlement variation with time for a load amplitude of 0.5 ton, loading frequency of 1 Hz, and R.D. of 30%, for tests on unreinforced and geocell-reinforced sand.

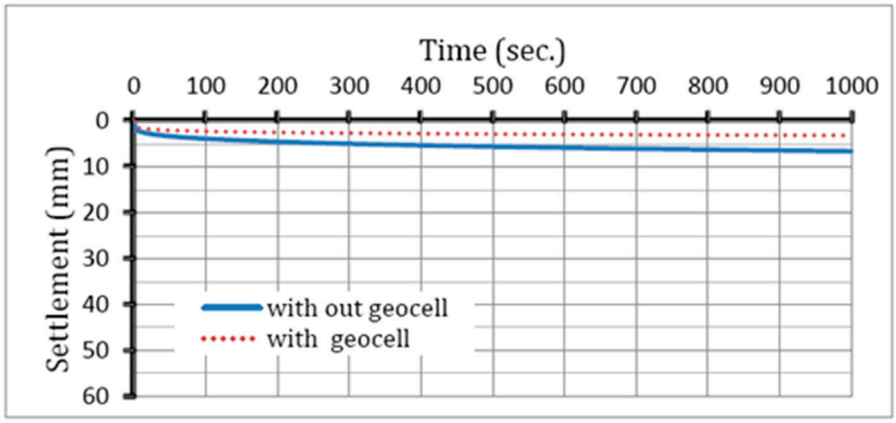


Figure 18. Surface settlement variation with time for a load amplitude of 0.5 ton, loading frequency of 0.5 Hz, and R.D. of 60%, for tests on unreinforced and geocell-reinforced sand.

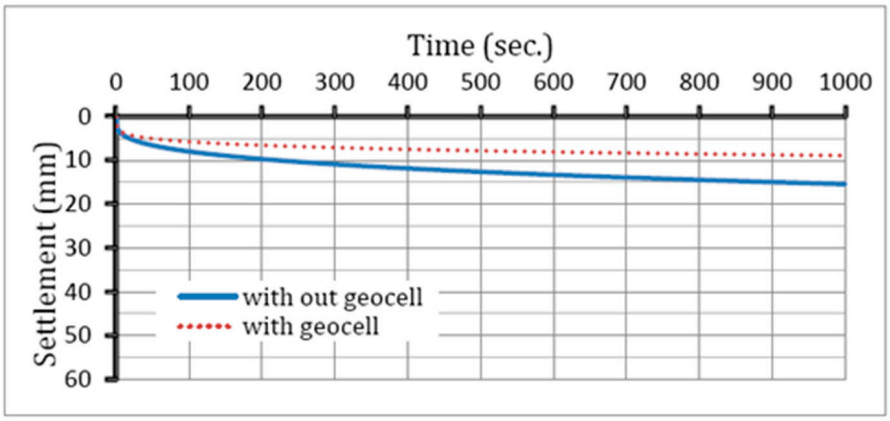


Figure 19. Surface settlement variation with time for a load amplitude of 1.0 ton, loading frequency of 0.5 Hz, and R.D. of 60%, for tests on unreinforced and geocell-reinforced sand.

The presence of geocell reinforcement significantly reduces the surface settlement in both soil states. In loose sand, the geocell reduces settlement by approximately 55–70% at a load amplitude equal to 0.5 ton and by 40–54% at an amplitude of 1.0 ton. On the other hand, the incorporation of geocell reinforcement significantly improved the performance of medium sand, ranging between 38 and 51% for the 0.5-ton load and 30 and 43% for the 1.0-ton load.

The observed improvement is mainly attributed to the high resistance of soil to composite stiffness resulting from the internal friction between the sand particles and the wall of geocells. This response delay reduces vertical compression and lateral spreading, which in turn limits settlement under dynamic loading.

3.3.2. Effect of Load Frequency

Figures 20–23 present the settlement-time behavior for the two relative densities under different loading frequencies and the same load amplitude. Overall, for both loose and medium sand, the settlement increases as the loading frequency value increases. Like the amplitude behavior, loose sand exhibits a greater rate of settlement increase compared with medium sand.

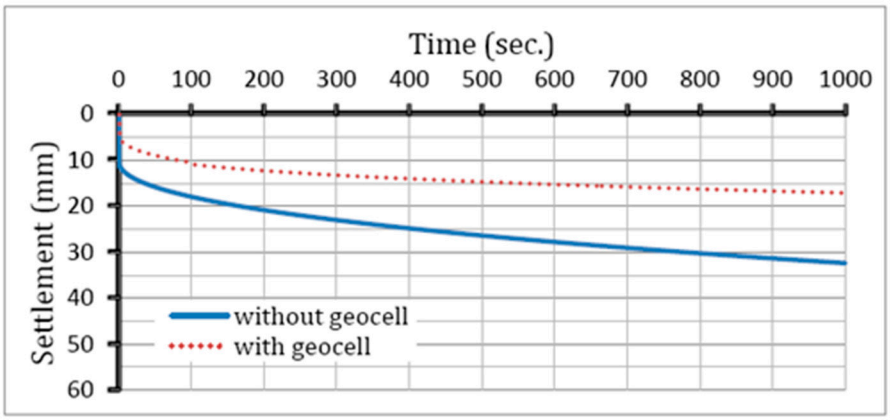


Figure 20. Surface settlement variation with time for a load amplitude of 1.0 ton, loading frequency of 1 Hz, and R.D. of 30%, for tests on unreinforced and geocell-reinforced sand.

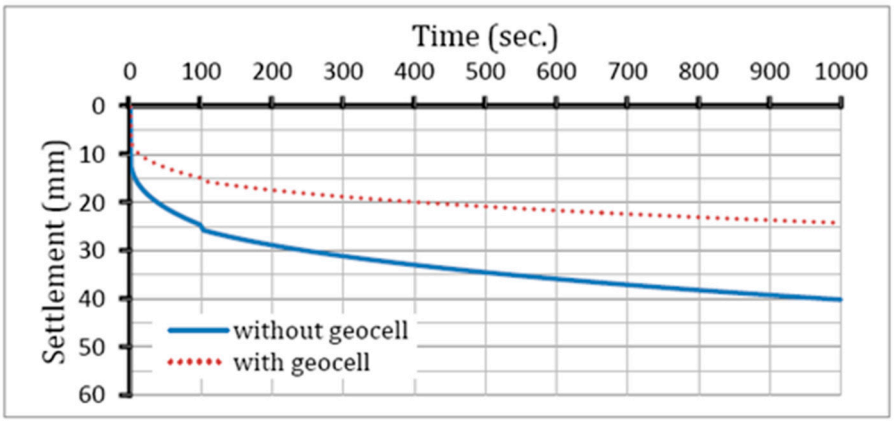


Figure 21. Surface settlement variation with time for a load amplitude of 1.0 ton, loading frequency of 2 Hz, and R.D of 30%, for tests on unreinforced and geocell-reinforced sand.

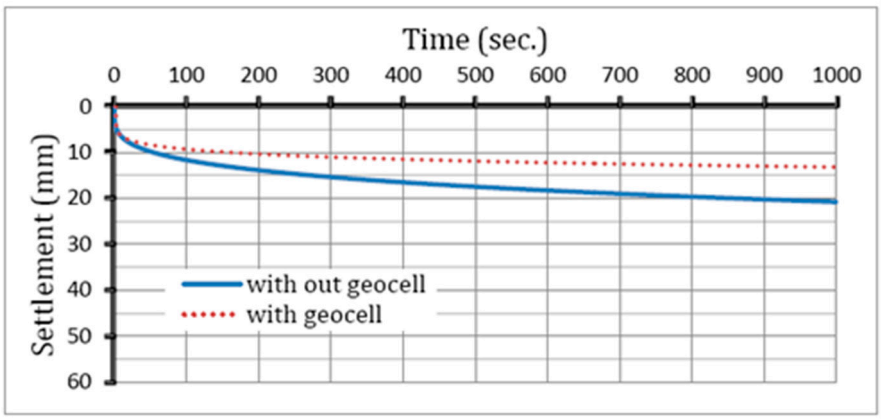


Figure 22. Surface settlement variation with time for a load amplitude of 1.0 ton, loading frequency of 1 Hz, and R.D. of 60%, for tests on unreinforced and geocell-reinforced sand.

When the frequency increases from 0.5 Hz to 2.0 Hz, the settlement of unreinforced sand rises by about 27%. The results also show a decrease in the effectiveness of geocell reinforcement as the frequency of load increases, even when the load amplitude remains constant. This reduction in effectiveness is due to the higher load cycle number applied within the same time interval, which impresses greater cyclic shear stresses on the soil–geocell system.

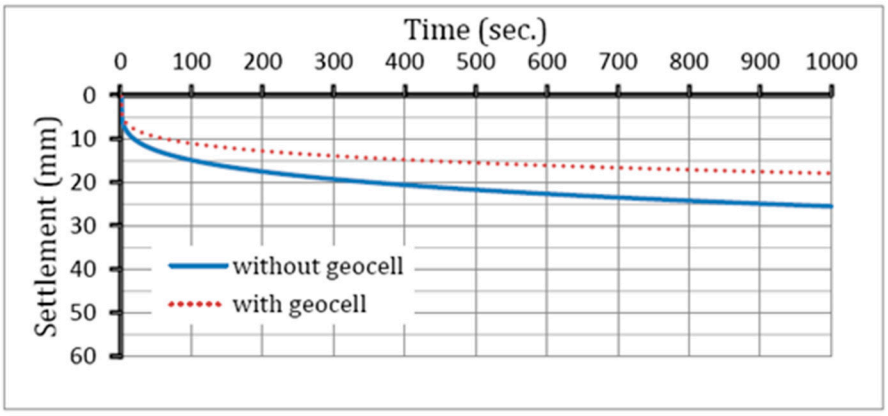


Figure 23. Surface settlement variation with time for a load amplitude of 1.0 ton, loading frequency of 2 Hz, and R.D. of 60%, for tests on unreinforced and geocell-reinforced sand.

Figure 24 demonstrates the variation in settlement with load amplitude for various relative densities. For any given frequency and density, the settlement increases consistently with increasing load amplitude, which confirms the strong dependence of deformation on soil stiffness and cyclic stress magnitude.

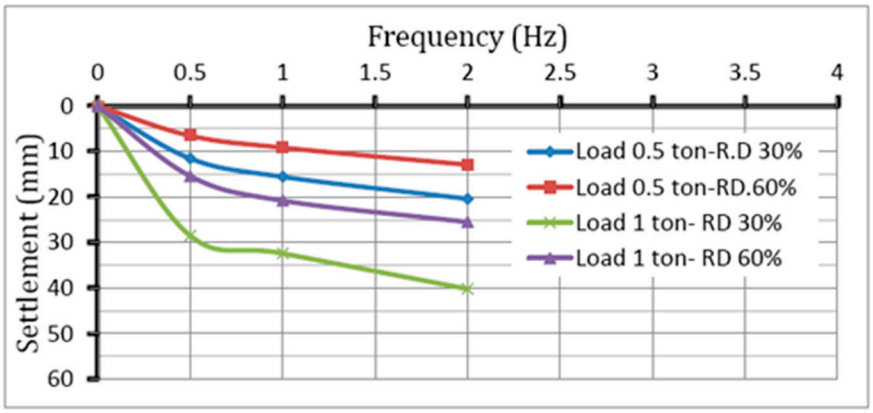


Figure 24. Relationship of surface settlement with loading frequency under different load amplitudes and relative densities.

The experimental results obtained in this study clearly explain the efficacy of geocell reinforcement in attenuating dynamic traffic loads transmitted through sandy soil subgrades. The following discussion integrates the observed behaviors, explains the underlying reinforcement mechanisms, and places the observed behaviors within the context of soil–reinforcement interaction under dynamic conditions.

- **Mechanism of Load Attenuation and Stress Distribution**

The primary mechanism through which geocell reinforcement improves soil performance is by transforming the localized load-bearing system into a wide-area, composite mat-like structure. When a dynamic load is applied to the surface of unreinforced sand, the stress bulb propagates downward with significant intensity, leading to high vertical pressures at depth and considerable surface settlement. The introduction of a geocell layer fundamentally alters this stress distribution. In addition, the geocell mattress, with its interconnected cells, provides all-around confinement to the infill soil. This confinement mobilizes hoop stresses within the cell walls and generates significant passive resistance from the surrounding encapsulated soil. As a result, the applied vertical load is not merely transferred downward but is also distributed laterally. This three-dimensional interaction creates a larger effective footing area, reducing the contact pressure on the underlying

subgrade soil. The observed reductions in vertical pressure at the depth of the pressure cell (up to 48% in loose sand) are a direct consequence of this load-spreading mechanism, effectively acting as a stress-dissipating layer.

- **Role of Soil Density and Reinforcement Effectiveness**

The results indicate that the degree of improvement offered by geocell reinforcement is more pronounced in loose sand than in medium-dense sand. For instance, the reduction in transmitted pressure decreased from 48% to 35% in loose sand as the load amplitude increased, while in medium sand, the reduction was lower, from 30% to 25%. A similar trend was observed for settlement reduction. This can be attributed to the initial state of the soil. Loose sand has a low initial stiffness and shear strength, making it highly susceptible to particle rearrangement and densification under dynamic loads. The geocell provides the necessary confinement that the loose sand inherently lacks, dramatically increasing its composite stiffness and bearing capacity. In contrast, medium-dense sand already possesses a higher interlocking of particles and internal friction angle, granting it a greater inherent resistance to deformation and stress transmission. Therefore, the relative improvement gained by adding reinforcement, while still significant, is less dramatic because the unreinforced soil already performs reasonably well.

- **Impact of Dynamic Loading Parameters: Amplitude and Frequency**

The study convincingly shows that the benefits of geocell reinforcement are influenced by the characteristics of the dynamic load itself.

- Load Amplitude: The decrease in improvement percentage with increasing load amplitude (from 0.5 ton to 1 ton) suggests that there is a limit to the geocell's capacity to redistribute stress. At higher loads, the shear stresses within the infill soil and the tensile forces in the geocell walls may approach their limits, leading to a reduction in the efficiency of the load-spreading mechanism. The system begins to behave more like the unreinforced case, albeit at a higher load threshold, indicating that the geocell is still providing a benefit but is operating closer to its ultimate capacity.
- Load Amplitude: The increase in both transmitted pressure and settlement with frequency is a classic dynamic soil response. A higher frequency means that more load cycles are applied in a given time, giving the soil less time to dissipate excess pore pressures (even in dry sand, inertial effects play a role) and undergo elastic recovery between cycles. This leads to an accumulation of plastic strain and a higher rate of settlement. The geocell's ability to reduce settlement diminishes at higher frequencies because the rapid, repeated loading challenges the soil–geocell composite's capacity to recover and re-mobilize its stiffness within each short cycle. The reinforcement still reduces the absolute settlement, but its relative efficiency compared to the static or low-frequency case decreases.

- **Settlement Reduction and Composite Stiffness**

The remarkable reduction in surface settlement (over 50% in many cases) is one of the most significant benefits of geocell reinforcement. This is a direct result of the increased composite stiffness of the soil–geocell layer. The reinforcement restricts the lateral yielding of the soil directly beneath the footing, forcing a larger volume of soil to participate in load bearing. This not only reduces immediate settlement but also mitigates the progressive accumulation of permanent settlement under repeated loading. The finding that settlement reduction was higher for loose sand further underscores the role of geocells in providing confinement where it is most needed.

- **Practical Effects and Design Concerns**

The findings of this study have direct practical implications for the design of transportation infrastructure, such as road embankments and rail beds over sandy subgrades. The use of geocell reinforcement can be considered a viable strategy for the following applications:

- Protection of Underlying Infrastructure: By significantly reducing the dynamic pressure transmitted to deeper soil layers, geocell-reinforced sand can potentially mitigate stress propagation toward underlying infrastructure, such as buried pipes and conduits, thereby reducing the risk of traffic-induced vibration effects in practical field applications.
- Reduction of Maintenance Requirements: The substantial reduction in surface settlement translates to less rutting and unevenness in pavements, leading to lower long-term maintenance costs and improved ride quality.
- Construction on Weak Sandy Soils: In loose sandy deposits, where traditional methods may require extensive excavation and replacement, geocell reinforcement offers an economical and efficient ground improvement technique capable of enhancing load-bearing performance under dynamic loading.

For optimal design, engineers should note that the benefit is maximized when the geocell is placed at a shallow depth (0.1 B, as used in this study) and has a width sufficient to ensure adequate lateral load distribution (3.2 B in this case). Furthermore, the results caution that while geocells are highly effective, their performance is not absolute and should be evaluated in the context of expected traffic load intensity (amplitude) and speed (which correlates with load frequency).

In conclusion, the geocell reinforcement system functions as a versatile and effective mechanical stabilizer that enhances the performance of sandy subgrades under dynamic traffic loading by confining the soil, increasing composite stiffness, and promoting a beneficial redistribution of stress, thereby mitigating both settlement and the transmission of dynamic forces to deeper layers.

4. Conclusions

Experimental studies have been conducted to evaluate the performance of geocell-reinforced sandy subgrades under dynamic loading conditions representative of traffic-induced excitation. Based on the comprehensive laboratory testing program, the following findings can be reported:

1. Comparison of the pressure results without and with geocells in loose and medium sand showed that the pressure transmitted to the soil subgrade reduced by approximately 25–48%, depending on the sand density and the applied load intensity. The maximum reduction was observed in loose sand under lower load amplitudes.
2. For unreinforced sand, the surface settling of the footing decreases as the sand relative density increases, while it increases when the load frequency and dynamic load amplitude increases. Furthermore, using geocells as reinforcement under all the different conditions resulted in a settlement reduction of more than 50%.
3. Increasing the relative density from 30% (loose) to 60% (medium), the vertical pressure and the surface settlement decreased by about 30% and 40%, respectively.
4. Overall, the reinforced soil layer with geocells leads to a positive decrease in dynamic response (transmitted dynamic pressure and surface settlement) for all soil states in varying percentages, as well as increasing soil strength and lowering the risks associated with dynamic traffic load.

Author Contributions: Conceptualization was performed by M.A., M.Y.F., H.Q., W.B.M.R., and B.Z.; Methodology was developed by M.A.; Validation process was carried out by M.A., H.Q., and M.Y.F.; Formal analysis was conducted by M.A. and H.Q.; Investigation was led by M.A., H.Q., and M.Y.F.; Resources were provided by M.A., H.Q., and M.Y.F.; Data curation was performed by M.A. and M.Y.F.; Original draft of the manuscript was prepared by M.A.; Review and editing were performed by M.A. and M.Y.F. All authors have read and agreed to the published version of the manuscript.

Funding: This research received no external funding.

Data Availability Statement: The data presented in this study is available on request from the corresponding author.

Conflicts of Interest: The authors declare no conflicts of interest.

References

1. Murillo, C.; Thorel, L.; Caicedo, B. Ground vibration isolation with geofoam barriers: Centrifuge modeling. *Geotext. Geomembr.* **2009**, *27*, 423–434. [CrossRef]
2. Xiao, J.; Wang, K.; Xue, L.; Liu, Z.; Bai, Y.; Sun, S.; Yang, F. Dynamic stress attenuation characteristics of geocell-reinforced railway subgrade. *Geosynth. Int.* **2023**, *31*, 555–567. [CrossRef]
3. Li, L.; Sun, K.; Xu, M.; Xiao, H.; Jiang, S. Study on the dynamic performance of heavy-load railway reinforced subgrade under flood condition. *Geotext. Geomembr.* **2025**, *53*, 985–998. [CrossRef]
4. Woods, R.D. Screening of surface wave in soils. *J. Soil Mech. Found. Div.* **1968**, *94*, 951–979. [CrossRef]
5. Thompson, D.J.; Jiang, J.; Toward, M.G.R.; Hussein, M.F.M.; Ntotsios, E.; Dijckmans, A.; Coulier, P.; Lombaert, G.; Degrande, G. Reducing railway-induced ground-borne vibration by using open trenches and soft-filled barriers. *Soil Dyn. Earthq. Eng.* **2016**, *88*, 45–59. [CrossRef]
6. Al-Haddad, S.A.; Fattah, M.Y.; Al-Ani, F.H. Protection of buried pipeline using geosynthetics—A review. *Geotech. Eng.* **2024**, *19*, 503–518. [CrossRef]
7. Zhou, H.; Wen, X. Model studies on geogrid-or geocell-reinforced sand cushion on soft soil. *Geotext. Geomembr.* **2008**, *26*, 231–238. [CrossRef]
8. Yang, X.; Han, J. Analytical model for resilient modulus and permanent deformation of geosynthetic-reinforced unbound granular material. *J. Geotech. Geoenviron. Eng.* **2013**, *139*, 1443–1453. [CrossRef]
9. Hegde, A.; Sitharam, T.G. 3-Dimensional numerical modelling of geocell reinforced sand beds. *Geotext. Geomembr.* **2015**, *43*, 171–181. [CrossRef]
10. Deshmukh, R.R.; Patel, S.; Shahu, J.T. Field assessment of improvement in composite modulus of geosynthetic-reinforced pavements. *Geosynth. Int.* **2021**, *28*, 624–633. [CrossRef]
11. Gao, B.; Liu, X.; Liu, J.; Song, L.; Shi, Y.; Yang, Y. Field characterization of dynamic response of geocell-reinforced aeolian sand subgrade under live traffic. *Appl. Sci.* **2023**, *13*, 864. [CrossRef]
12. Zhao, Y.; Lu, Z.; Liu, J.; Zhang, J.; Yao, H. Influence of different infill materials on the performance of geocell-reinforced cohesive soil beds. *Sci. Rep.* **2023**, *13*, 12330. [CrossRef] [PubMed]
13. Cheng, B.; Huang, J.; Wang, H.; Li, X. Influences of Geocell Reinforcement on Shear Strength of Railway Roadbeds. *Transp. Res. Rec.* **2024**, *2678*, 1029–1045.
14. Alotaibi, E.; Omar, M.; Shanableh, A.; Zeiada, W.; Fattah, M.Y.; Tahmaz, A.; Arab, M.G. Geogrid bridging over existing shallow flexible PVC buried pipe–Experimental study. *Tunn. Undergr. Space Technol.* **2021**, *113*, 103945. [CrossRef]
15. Kumar, A.; Singh, A.P.; Chatterjee, K. Ground improvement using geocells to enhance trafficability in desert soils. *Geomech. Eng.* **2019**, *19*, 71–78.
16. Song, F.; Liu, H.; Yang, B.; Zhao, J. Large-scale triaxial compression tests of geocell-reinforced sand. *Geosynth. Int.* **2019**, *26*, 388–395. [CrossRef]
17. Venkateswarlu, H.; Hegde, A. Effect of influencing parameters on the vibration isolation efficacy of geocell reinforced soil beds. *Int. J. Geosynth. Ground Eng.* **2020**, *6*, 16. [CrossRef]
18. Shin, E.C.; Das, B.M.; Lee, E.S.; Atalar, C. Bearing capacity of strip foundation on geogrid-reinforced sand. *Geotech. Geol. Eng.* **2002**, *20*, 169–180. [CrossRef]
19. Tafreshi, S.M.; Khalaj, O. Laboratory tests of small-diameter HDPE pipes buried in reinforced sand under repeated-load. *Geotext. Geomembr.* **2008**, *26*, 145–163.
20. Ismaeil, M.S. Influence of Geogrid Reinforcement of Sand in Transfer of Dynamic Loading to Underground Structure. Master's Thesis, Building and Construction Engineering Department, University of Technology, Baghdad, Iraq, 2015.

21. Venkateswarlu, H.; Ujjawal, K.N.; Hegde, A. Laboratory and numerical investigation of machine foundations reinforced with geogrids and geocells. *Geotext. Geomembr.* **2018**, *46*, 882–896. [CrossRef]
22. Azzam, W.R. Utilization of the confined cell for improving the machine foundation behavior-numerical study. *J. GeoEngin.* **2015**, *10*, 17–23.
23. Duong, T.V.; Cui, Y.J.; Tang, A.M.; Dupla, J.C.; Canou, J.; Calon, N.; Robinet, A. Investigating the mud pumping and interlayer creation phenomena in railway sub-structure. *Eng. Geol.* **2014**, *171*, 45–58. [CrossRef]
24. Hasnayn, M.M.; McCarter, W.J.; Woodward, P.K.; Connolly, D.P.; Starrs, G. Railway subgrade performance during flooding and the post-flooding (recovery) period. *Transp. Geotech.* **2017**, *11*, 57–68. [CrossRef]
25. Indraratna, B.; Korkitsuntornsan, W.; Nguyen, T.T. Influence of Kaolin content on the cyclic loading response of railway subgrade. *Transp. Geotech.* **2020**, *22*, 100319. [CrossRef]
26. Pokharel, S.K.; Han, J.; Manandhar, C.; Yang, X.; Leshchinsky, D.; Halahmi, I.; Parsons, R.L. Accelerated pavement testing of geocell-reinforced unpaved roads over weak subgrade. *Transp. Res. Rec.* **2011**, *2204*, 67–75.
27. Yang, X.; Han, J.; Pokharel, S.K.; Manandhar, C.; Parsons, R.L.; Leshchinsky, D.; Halahmi, I. Accelerated pavement testing of unpaved roads with geocell-reinforced sand bases. *Geotext. Geomembr.* **2012**, *32*, 95–103. [CrossRef]
28. *ASTM D854-14*; Standard Test Method for Specific Gravity of Soil Solids by Water Pycnometer. ASTM International: West Conshohocken, PA, USA, 2016.
29. *ASTM D422-63*; Standard Test Method for Particle-Size Analysis of Soils. ASTM Standards: West Conshohocken, PA, USA, 2007.
30. *ASTM D2487-17*; Standard Practice for Classification of Soils for Engineering Purposes (Unified Soil Classification System). American Society for Testing and Materials: West Conshohocken, PA, USA, 2023.
31. *ASTM D4253-20*; Standard Test Methods for Maximum Index Density and Unit Weight of Soils Using a Vibratory Table. ASTM International: West Conshohocken, PA, USA, 2020.
32. *ASTM D4254-20*; Standard Test Methods for Minimum Index Density and Unit Weight of Soils and Calculation of Relative Density. ASTM International: West Conshohocken, PA, USA, 2020.
33. *ASTM D3080-23*; Standard Test Method for Direct Shear Test of Soils Under Consolidated Drained Conditions. Annual book of ASTM standards; ASTM Standards: West Conshohocken, PA, USA, 2003; 4p.
34. Dash, S.K.; Krishnaswamy, N.R.; Rajagopal, K. Bearing capacity of strip footings supported on geocell-reinforced sand. *Geotext. Geomembr.* **2001**, *19*, 235–256.
35. Fattah, M.; Mohammed Redha, W.B. Protection of flexible pipes from dynamic surface stresses by Geocell-reinforced sand backfill. *Int. J. Min. Geo-Eng.* **2022**, *56*, 61–66.
36. Tafreshi, S.M.; Dawson, A.R. Behaviour of footings on reinforced sand subjected to repeated loading–Comparing use of 3D and planar geotextile. *Geotext. Geomembr.* **2010**, *28*, 434–447. [CrossRef]
37. Al-Ameri, A.I. Transient and Steady State Response Analysis of Soil Foundation System Acted upon by Vibration. Ph.D. Thesis, College of Engineering, Civil Engineering Department, University of Baghdad, Baghdad, Iraq, 2014.
38. Fattah, M.Y.; Al-Mosawi, M.J.; Al-Ameri, A.F. Vibration response of saturated sand-foundation system. *Earthq. Struct.* **2016**, *11*, 83.

Disclaimer/Publisher's Note: The statements, opinions and data contained in all publications are solely those of the individual author(s) and contributor(s) and not of MDPI and/or the editor(s). MDPI and/or the editor(s) disclaim responsibility for any injury to people or property resulting from any ideas, methods, instructions or products referred to in the content.